

Muscle Architecture of Leg Muscles: Functional and Clinical Significance

Gurpreet Kaur

LN Medical College, Bhopal, India

Manal M. Khan

All India Institute of Medical Sciences, Bhopal, India

Rekha Lalwani

All India Institute of Medical Sciences, Bhopal, India

Sunita Arvind Athavale*

All India Institute of Medical Sciences Bhopal, India

Abstract. Background. Architectural properties of the muscles are the prime predictors of functional attributes and force-generating capacity of the muscles. This data is vital for musculoskeletal modelling and selecting the appropriate muscle–tendon units for tendon transfers.

Cadaveric data for architectural properties is the gold standard and primary input for musculoskeletal modelling. There is a paucity of these datasets, especially in the leg muscles.

Methods. Sixty muscles of the anterior and lateral compartments from twelve formalin-fixed lower limbs were studied for gross architecture, including the peculiar fibre arrangements and architectural properties of muscles. Muscle weight, muscle length, fibre length, pennation angle and sarcomere length were measured. Normalised fibre length, fibre length to muscle length ratio (FL/ML ratio), and the physiological cross-sectional area (PCSA) were calculated from the obtained data.

Results. Muscles displayed a combination of architectural strategies and were partly fusiform and partly pennate. The tibialis anterior and peroneus longus were the heaviest muscles in their respective compartments and showed more extensive origin from the nearby deep facial sheets.

Long fibre length and less pennation angle were seen in muscles of the extensor compartment. Potential muscle power was highest in the tibialis anterior and peroneus longus and least in the extensor hallucis longus.

Conclusions. Arching of the foot and eversion are peculiar to humans and recent in evolution. Due to the functional demand of maintaining the medial longitudinal arch and eversion, the tibialis anterior and peroneus longus have more muscle weight and larger physiological cross-sectional area and are potentially more powerful.

Extensor compartment muscles were architecturally more suited for excursions because of the long fibre length and less pennation angle.

This study contributes baseline normative data for musculoskeletal modelling platforms and simulation tools – an emerging area in biomechanics and tendon transfers.

Keywords: Medial longitudinal arch, Musculoskeletal modelling, Pennation angle, Sarcomere length, Tendon transfer.

* Corresponding author: Sunita Arvind Athavale, All India Institute of Medical Sciences Bhopal, India. E-mail: sunita.anatomy@aiimsbhopal.edu.in

Received: 03/06/2023. Revised: 24/07/2023. Accepted: 30/08/2023

Copyright © 2023 Gurpreet Kaur, Rekha Lalwani, Manal M. Khan, Sunita Arvind Athavale. Published by Vilnius University Press. This is an Open Access article distributed under the terms of the Creative Commons Attribution License, which permits unrestricted use, distribution, and reproduction in any medium, provided the original author and source are credited.

Kojų raumenų architektūra: funkcinė ir klinikinė reikšmė

Santrauka. Kontekstas. Architektūrinės raumenų savybės yra pirminės svarbos požymiai, kuriais remiantis galima prognozuoti funkcinis raumenų požymius ir raumenų gebėjimą kurti galią. Šie duomenys gyvybiškai svarbūs raumenų ir kaulų (skeleto) modeliavimui atlikti bei parinkti tinkamus raumens ir sausgyslių derinius, kai atliekamas sausgyslių perkėlimas.

Raumenų ir kaulų (skeleto) modeliavimas tiriant raumenų architektūrinės savybes yra paremtas mirusiųjų tyrimais. Tokie tyrimai, manoma, atitinka aukščiausius standartus ir yra svarbus duomenų šaltinis. Tačiau tokių duomenų rinkinių kiekis yra menkas, ypač kalbant apie kojų raumenis.

Metodai. Buvo ištirta 60 paimtų iš dvylikos formaline preparuotų apatinių galūnių priekinio ir šoninio segmentų raumenų siekiant išanalizuoti bendrąją architektūrą. Tirtas konkrečių pluoštų išsidėstymas ir architektūrinės raumenų savybės. Matuota raumenų svoris, raumenų ilgis, pluošto ilgis, penacijos kampas ir sarkomero ilgis. Iš gautų duomenų apskaičiuotas normalizuotas pluošto ilgis, pluošto ilgio ir raumens ilgio santykis (FL/ML santykis) bei fiziologinio skerspjuvio plotas (PCSA plotas).

Rezultatai. Raumenys atskleidė įvairių architektūrinių strategijų derinį. Jie buvo dalinai verpstės formos, dalinai įstrižinis. *Tibialis anterior* ir *peroneus longus* buvo sunkiausi savo segmentų raumenys.

Ekstensoriaus segmento raumenų buvo nustatytas didesnis pluošto ilgis bei mažesnis penacijos kampas. Didžiausią potencialią galią generavo *tibialis anterior* ir *peroneus longus* raumenys, o mažiausia buvo *extensor hallucis longus* raumens galia.

Išvados. Pėdos išlinkimas ir eversija yra būdinga tik žmonėms. Tai yra naujas reiškinys evoliucijoje. Dėl funkcinės būtinybės išlaikyti medialinę išilginę arką ir eversiją *tibialis anterior* ir *peroneus longus* raumenys pasižymi didesniu svoriu ir didesniu fiziologiniu skerspjuvio plotu. Potencialiai tai yra galingesni raumenys.

Ekstensoriaus segmento raumenys architektūriškai yra tinkamesni ekskursijos, nes jų pluošto ilgis yra didesnis, o penacijos kampas yra mažesnis.

Šis tyrimas suteikia pradinių norminių duomenų raumenų ir kaulų modeliavimo platformoms bei simuliacijų įrankiams, kurie yra vis labiau populiarėjanti biomechanikos ir sausgyslių perkėlimo tyrimų sritis.

Raktažodžiai: Medialinė išilginė arka, raumenų ir kaulų modeliavimas, penacijos kampas, sarkomero ilgis, sausgyslės perkėlimas.

Introduction

Structure-function relationships in skeletal muscles have been examined quite extensively microscopically. However, less attention has been paid to the macroscopic arrangement of muscle fibres, known as muscle architecture. Muscle architecture can be defined as “the arrangement of muscle fibres within a muscle relative to its axis of force generation” [1]. Architectural properties of muscles are considered good indicators of force generation and potential for excursion [2]. Architectural differences are thus the best predictors of force generation [1].

Gans emphasised that the arrangement of fibres in a muscle reflects its function. Parallel fibered muscles are primitive and simplest, providing maximum excursion. The pennate arrangement of fibres allows more fibres to be packed in a muscle, increasing the cross-sectional area and potential force production [3].

The principles of tendon transfers have been refined over time. It is now understood that properties of muscles like expendability, adequate strength and excursion of the transferred unit are of prime importance [1]. When choosing an adequate muscle-tendon unit to be transferred, the treating physician has to ensure that the unit is expendable, meaning there must be another muscle-tendon unit that can perform the donor unit’s original function. The muscle-tendon unit being transferred should have adequate strength and excursion to be effective [4].

In the last two decades, attempts have been made to study the architectural properties of muscles frequently used in tendon or muscle transfers. However, most available studies have focussed on the

muscle architecture of forearm muscles [5-9], and relatively few studies have focussed on leg muscles [10-12].

In their recent works, Kissane et al. have demonstrated that the muscle architectural properties are key inputs to the central nervous system, and the muscle spindle abundance is significantly correlated with the muscle architecture (fibre length, pennation angle and physiological cross-sectional area), thus modulating locomotion [13,14].

Knowledge of baseline architectural properties shall also help in reliably measuring the outcome of therapeutic interventions targeted at improving muscle power which is dependent on architectural properties [15].

Computational modelling and in-silico studies is an emerging field of biomechanics. Cadaveric and experimental data is the primary input for such modelling. Human muscle architecture is also investigated using ultrasound and MRI [16-18]. However, due to the limitations of current-generation imaging facilities, the gold standard for muscle architecture data remains the dissection of a cadaver [12]. Therefore, the present study intends to describe the gross architecture, including the peculiar fibre arrangements and architectural properties of muscles in the anterior and lateral leg compartments.

Material and methods

This was a descriptive, cross-sectional, exploratory cadaveric study on twelve formalin-fixed embalmed lower limbs in the Department of Anatomy. Gross architecture and architectural properties of the muscle of the anterior and lateral compartments of the leg were studied.

Lower limbs with any evidence of congenital/acquired anatomic abnormalities/deformity were excluded.

Muscles were observed and dissected along its tendon to study the gross architecture. The shape of the muscle and fibre pattern was recorded in terms of pennation. The special origin of fibres was also recorded.

The following parameters were measured in architectural analysis: a) muscle weight, b) muscle length, c) fibre length, d) pennation angle and e) sarcomere length. After removing the surrounding fascia and fat tissues, the muscles were harvested intact (from the most proximal origin to the most distal tendon attachment). They were stored in 1x phosphate-buffered saline for 24–48 hours before architectural measurements. Muscle specimens were removed from the buffer and gently blotted dry. The following constituents formed 1x phosphate-buffered saline – 800 millilitres of distilled water, 8 g of sodium chloride (NaCl), 0.2 g of potassium chloride (KCl), 1.44 g of sodium hydrogen phosphate (Na_2HPO_4), 0.24 g of potassium dihydrogen phosphate KH_2PO_4 , pH (potential of hydrogen) adjusted to 7.4 with hydrogen chloride (HCl) and distilled water added to a total volume of 1 litre [19].

Muscle weight (MW) was recorded using a Digital Weighing machine with measurements of up to 2 decimals. The muscle was weighed, but the weight was not corrected for formaldehyde fixation. The external tendons, connective tissue and fat were removed before weighing.

Muscle length (ML) was measured as the distance from the origin of the most proximal muscle fibres to the insertion of the most distal muscle fibres by thread and centimetre scale.

Pennation angle (PA) was measured with a goniometer; a protractor was kept over it for more precision. Pennation angle was obtained from the proximal, middle, and distal muscle portions and averaged to yield one value per muscle.

Depending on the morphology of the muscle, pennation angle was calculated from the unipennate and bipennate parts of the muscle (Figure 1). Circumpennate portions were not included as calculation of pennation was not possible with the methodology used. The mean of pennation angle of different muscle parts was considered the final value.

Muscle fibre length. The muscles were placed in 20% nitric acid to partially digest the connective tissue surrounding the muscles and allow the separation of approximately 0.1mm thick bundles.



Figure 1. Showing the measurement of pennation angle measurement with a goniometer.



Figure 2. Showing measurement of fibre length with digital vernier calliper.

The average digestion time was 48 hours. Thin fibre bundles were separated, kept straight without stretching, and length was measured with a digital vernier calliper (Figure 2). The muscle was divided into three equal parts. Three readings were taken from the centre of each part. The average of the three readings was taken as the final value.

Sarcomere length: After acid digestion, individual fibres were removed with forceps and with the aid of a microscope. Sections of fibre approximately 5 mm long were mounted on a micrometry slide using isotonic saline (Figure 3). The muscle was divided into three equal parts. Three sections were taken from the centre of each part. Digital images of the fibre sections were taken from a light microscope at 100x magnification. Two readings were recorded from one section, so a total of six readings were recorded from one muscle.

Fibre length was normalised to compensate for natural fibre length variation simply because muscles were fixed at different joint angles. For normalisation of fibre length, the sarcomere length within a specimen was measured, and a standard sarcomere length (2.7 μm) was selected. Then all raw fibre lengths were normalised using the following equation:

$$FL(\text{cm}) = \frac{FL'(\text{cm}) \times SL(\mu\text{m})}{SL'(\mu\text{m})},$$

FL – normalized fibre length, FL' – raw fibre length, SL – standard sarcomere length (2.7 μm), SL' – experimentally measured sarcomere length [9].

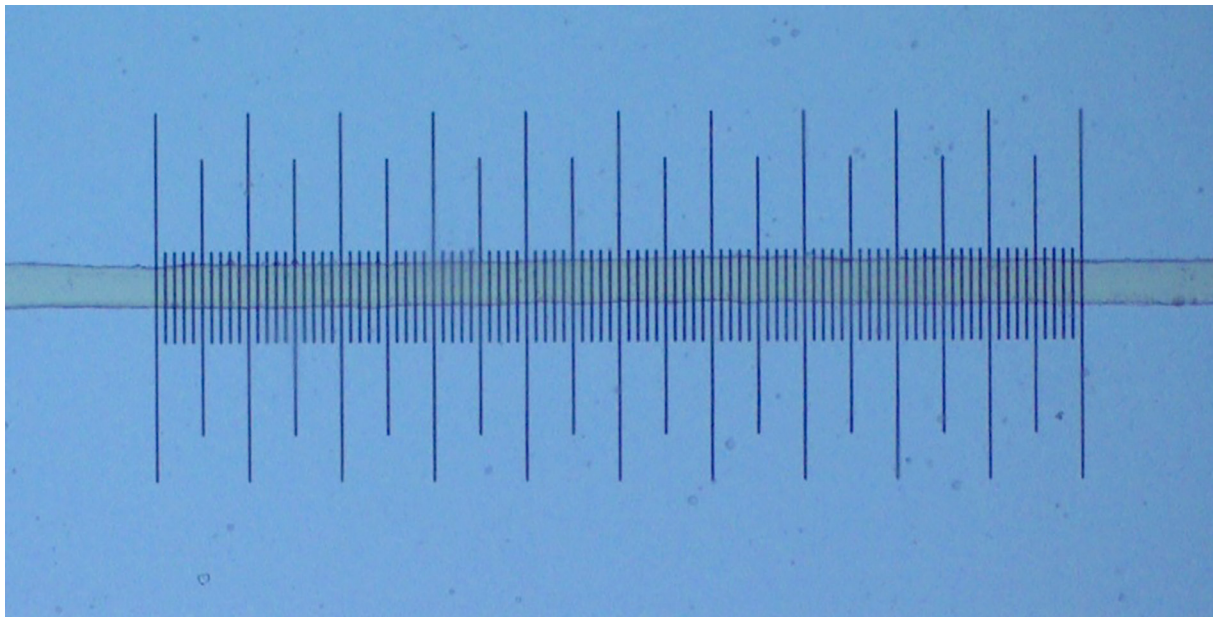


Figure 3. Showing the micrometry of one muscle fibre at a scale of 10x.

Fibre length to muscle length ratio (FL/ML ratio) was calculated by dividing fibre length by muscle length.

The physiological cross-sectional area (PCSA) was calculated using the following equation:

$$PCSA(\text{cm}^2) = \frac{MW(\text{g}) \times \cos\theta}{\rho\left(\frac{\text{g}}{\text{cm}^3}\right) \times FL(\text{cm})}$$

θ is the surface pennation angle, and ρ is muscle density (1.056 g cm^{-3}).

Fibre length / muscle weight ratio and **PCSA / muscle weight ratio** were also calculated.

Findings of all study parameters of architectural properties were subjected to Descriptive statistics by SPSS version 21.

Results

Gross architecture

The gross architecture in the muscles of the anterior and lateral leg compartments varied within and across the compartments. It was observed usually that the muscle had a uniform fusiform pattern in their proximal fourth or proximal third. Here the muscle fibre ran almost parallel to the long axis of the muscle. In the distal two-thirds or three-fourths, the muscles assumed a pennate pattern (unipennate/bipennate/circumpennate), arranging themselves around an aponeurosis which was initially in the form of broad aponeurosis and, when traced distally, thickened to form a tendon.

The gross architecture of individual muscles, as observed in the present study, was as follows.

Muscles of lateral compartment

The upper third to an upper fourth of each muscle was fusiform, and the remaining portion was variably pennate (Fig. 4 i-v).

Peroneus longus. The lower three-fourths was unipennate, where the fibres arising from bony attachment as well as fascial covering of the peroneus longus converge towards the intramuscular aponeurosis (Fig. 4 i & 5).

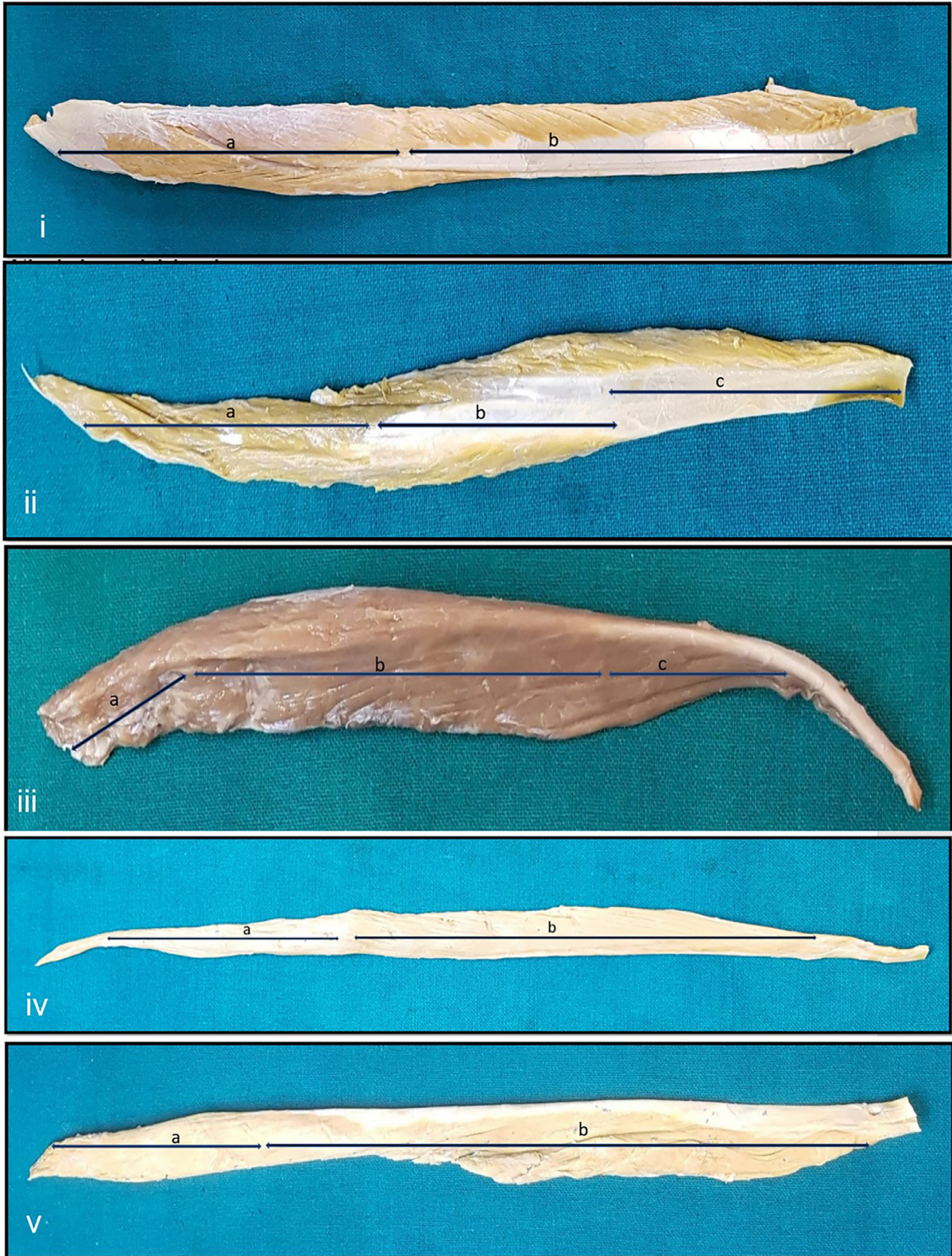


Fig. 4 (i-v) shows the muscles of the anterior and lateral compartments as visualised from their superficial surface. Arrow represents the fusiform portion, and arrows b and c the pennate portions. 4 (i) – peroneus longus; 4 (ii) – peroneus brevis; 4 (iii) – tibialis anterior; 4 (iv) – extensor hallucis longus; 4 (v) – extensor digitorum longus and peroneus tertius (EDL and PT).

Fig. 2 shows the origin of muscle fibres from the fascia covering the muscle (arrowheads). Fibres are seen inserting into the intramuscular tendon.

Peroneus brevis. Was bipennate in the middle one-third and unipennate in the lower one-third (Fig. 4 ii).

Muscles of anterior compartment

Tibialis anterior

The muscle was triangular in cross-section, with the base directed superficially. In the middle half, fibres converge onto the intramuscular aponeurosis from all aspects, making it circumpennate. In the lower one-fourth, the muscle was unipennate (Fig. 4 iii).

Extensor hallucis longus

The intramuscular aponeurosis is uniform throughout, with a pointed apex. The lower three-fourths of the muscle was unipennate (Fig. 4 iv).

Extensor digitorum longus and peroneus tertius (EDL and PT)

The extensor digitorum longus and peroneus tertius muscle belly were conjoint in the upper part. The distal two-thirds of the muscle is separated into five intramuscular aponeuroses with unipennate fibres inserted into them (Fig. 4 ii).

Architectural analysis of muscles of anterior and lateral compartments

Twelve samples were taken for the measurements of each muscle. Average values for all the architectural parameters of individual muscles are compiled in Table 1. Peroneus tertius was considered a part of the extensor digitorum longus, as the muscle was inseparable from the extensor digitorum longus.

Architectural analysis

Peroneus longus measured twice as heavy compared to peroneus brevis. In the anterior compartment, the tibialis anterior is twice as heavy as extensor digitorum longus and four times that of extensor hallucis longus.

Extensor digitorum longus was the longest muscle closely followed by tibialis anterior.

Pennation angle for anterior compartment muscles was comparatively less than muscles of lateral compartment ranging from 10 to 14 degrees. In the lateral compartment, pennation angle for peroneus longus and peroneus brevis is similar around 18 degrees.

Muscles of the anterior compartment have long fibre length owing to more excursion produced by the muscles. These muscles' fibre length was almost double compared to the lateral compartment. Tibialis anterior has a high physiological cross-sectional area, whereas extensor hallucis longus and extensor digitorum longus have low physiological cross-sectional area among leg muscles.

Sarcomere length for tibialis anterior and extensor hallucis longus was lower, whereas for extensor digitorum longus, peroneus longus and peroneus brevis, it was higher.

Discussion

Architectural properties of the muscles are the best indicators of muscle function. The muscle power and excursion are determined by properties like muscle weight, fibre length, pennation angle and physiological cross-sectional area [1, 3, 20, 21]. The muscles of the anterior and lateral compart-

Table 1. Architectural parameter of muscles of extensor and lateral leg compartments.

	Muscle Weight	Muscle Length	Pennation Angle	Sarcomere Length	Fibre Length	Normalized Fibre Length	Fibre Length/Muscle Length Ratio	Physiological Cross-Sectional Area (PCSA)	Fibre Length/Muscle Weight Ratio	Physiological Cross-Sectional Area (PCSA)/Muscle Weight
Tibialis Anterior	76.18±24	31.03±3	13.75±2	2.1±0.4	8.25±1.2	11.16±3.5	0.26±0.04	8.44±1.9	0.11±0.02	0.11±0.02
Extensor Hallucis Longus	18.73 ± 4	26.7 ± 4	10.16 ± 2	1.94 ± 0.2	8.82 ± 1.7	12.49 ± 3.1	0.33 ± 0.06	2.06 ± 0.7	0.50 ± 0.17	0.10 ± 0.02
Extensor Digitorum Longus & Peroneus Tertius	38.65 ± 9.8	33.31 ± 4.8	10.71 ± 2.2	3.23 ± 0.9	7.66 ± 1.2	6.80 ± 1.78	0.23 ± 0.03	4.78 ± 1.37	0.20 ± 0.05	0.12 ± 0.02
Peroneus Longus	50.35 ± 16	28.95 ± 3	18.87 ± 5	3.4 ± 0.2	4.08 ± 0.6	3.17 ± 0.38	0.14 ± 0.03	11.29 ± 4	0.08	0.22 ± 0.03
Peroneus Brevis	23.96 ± 7.2	23.08 ± 2.8	18.09 ± 5.9	3.87 ± 0.75	3.54 ± 0.6	2.53 ± 0.62	0.15 ± 0.02	6.11 ± 1.8	0.15 ± 0.05	0.25 ± 0.03

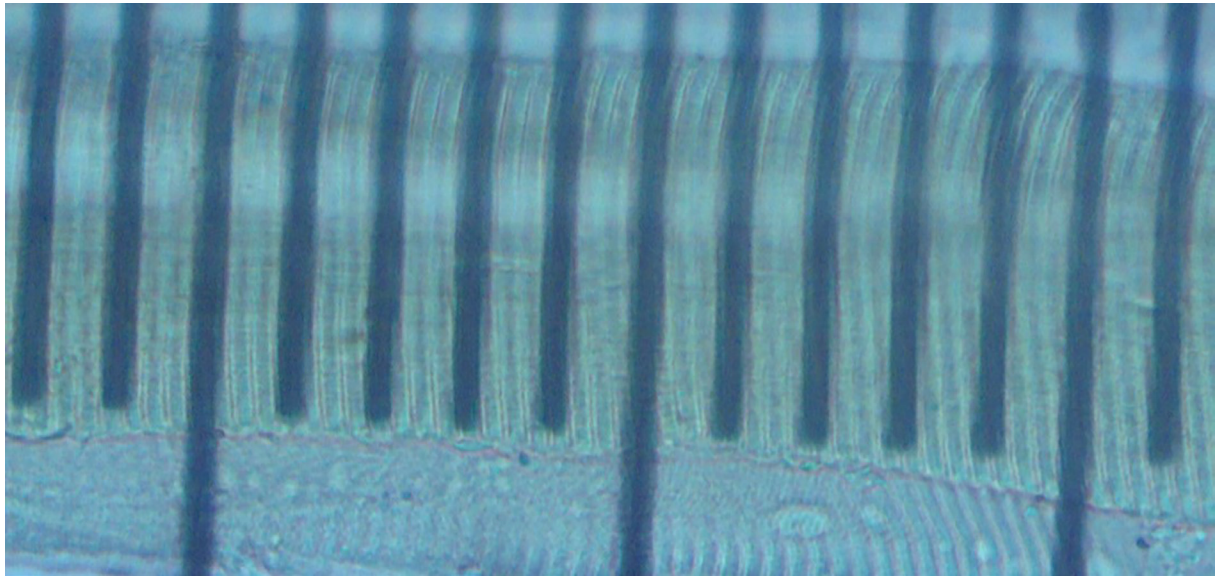


Figure 5. Showing 2.5 sarcomere in 0.01 mm of micrometry scale.

ments exhibit a combination of architectural strategies to optimise the function ascribed to them. This was evident in all the muscles as they combined fusiform (parallel) and pennate arrangement. The parallel fibres determine the excursion of the muscles, whereas the pennation adds the number of muscle fibres, and thus the resultant force.

Architecture properties showed a peculiar trend as follows.

Tibialis anterior was 2 to 4 times heavier than the other extensor compartment muscles. This indicates more powerful muscle action.

The pennation angle of the extensor compartment muscles was smaller and fibre length and normalised fibre length were larger, which indicates their predominant role in the excursion [2].

The physiological cross-sectional area is the summation of the force exerted by individual muscle fibres and determines the force generation capacity of the muscle–tendon units [3]. Pennation results in an increased number of muscle fibres, but there is a resultant loss of force which is compensated by increased physiological cross-sectional area to achieve a critical balance of enhancing the ultimate action of the muscle.

While physiological cross-sectional area determines the force generation capacity and fibre length relative velocity of contraction, muscle power is the product of force and velocity [21]. Hence, the potential muscle power in descending order was: tibialis anterior followed by peroneus longus, extensor digitorum longus, and peroneus tertius, and the least powerful was extensor hallucis longus. This underscores their role in maintaining the arch and eversion of the foot. It was observed that the muscles tibialis anterior, extensor digitorum longus, peroneus longus and peroneus brevis also originated considerably from the nearest available deep facial sheets. This was most prominently observed in the case of tibialis anterior and peroneus longus.

The muscle weight of the tibialis anterior and the pennation angle of peroneus tertius showed high variability both in our study and that of Ward et al. (2009) [11]; however, fibre length and physiological cross-sectional area were less variable. This may be because these parameters are independent of individual anthropometric data. Our findings conformed to those of Ward et al. (2009) in those parameters [11].

In a recent in-vivo study, Charles et al. (2019) have studied muscle architectural properties with the help of Diffusion Tensor Imaging (DTI) in young adults and have underscored the importance

of architectural properties for muscular skeletal modelling. However, they have also accepted this method's limitations in terms of its consistency and for measuring fiber length, sarcomere length and pennation angle [27].

Musculoskeletal modelling is being increasingly used to create virtual models of the human biological system. These models are used for in-silico biomechanical analysis viz. normal and abnormal gait analysis, joint and ligament forces and help predict the success of novel and ongoing surgical and rehabilitation modalities [28].

Architectural properties of the anterior and lateral compartments have not been extensively studied. Cadaveric data is a gold standard for obtaining the normative values for the architectural properties of the muscles for musculoskeletal modelling. Amongst the available cadaveric studies, Ward et al. (2009) have conducted on 21 limbs, while other studies are restricted to only 2-3 limbs [8,11, 20-26]. There seems to be a paucity of cadaveric data, The study will be an addition to the baseline normative data for musculoskeletal modelling and simulation.

The result of this study will aid plastic and orthopaedic surgeons in choosing the appropriate muscle-tendon unit as per requirement in cases of tendon and muscle transfers. When choosing an adequate muscle-tendon unit to be transferred, the treating physician has to ensure that the unit is expendable, meaning there must be another muscle-tendon unit that can perform the donor unit's original function. The muscle-tendon unit being transferred should have adequate strength and excursion to be effective [4].

Musculoskeletal system is very adaptive to interventions like muscle strengthening, stretching, constraint induced training, treadmill training, and functional electrical stimulation. In clinical conditions like cerebral palsy even pharmacological interventions targeting the central nervous system can alter the architectural properties. The knowledge of baseline architectural properties would help in reliably measuring the response to such interventions [15].

Arching of foot and eversion are peculiarly human traits and are still under evolution. Consequently, the muscles engaged in these actions are expected to be more powerful. Besides acting as dorsiflexors, the extensor compartment muscles have additional functions, e.g., tibialis anterior maintains the medial longitudinal arch and peroneus tertius part of extensor digitorum longus acts as an evertor. Similarly, amongst the lateral compartment muscles, peroneus longus, besides being an evertor, also maintains the medial longitudinal arch. The architectural properties of these muscles and their relative potential muscle power conform to their roles.

Conclusion

The architectural properties of tibialis anterior make it suitable for force as well as excursion. Extensor muscles are more suited for the excursion. The potential muscle power in descending order was tibialis anterior > peroneus longus > extensor digitorum longus > peroneus brevis > extensor hallucis longus (TA > PL > EDL > PB > EHL). Muscles supporting the medial longitudinal arch were potentially more powerful followed by evertors.

Limitations

The cadaveric limbs belonged to male cadavers only, owing to paucity of female cadaveric limbs available for study.

The pennation angle was calculated from the unipennate and bipennate parts of the muscle. Circumpennate portions were not included as calculation of pennation was not possible with the methodology used.

Conflict of interest statement

None. The Authors confirm that this research article entitled “Muscle Architecture of Leg Muscles: Functional and Clinical Significance” is original and has been published only in a pre-print service (Research Square): <https://doi.org/10.21203/rs.3.rs-2071159/v1>

References

1. Sammer DM, Chung KC. Tendon transfers part I: principles of transfer and transfers for radial nerve palsy. *Plast Reconstr Surg*. 2009;123(5):169e-177e. doi:10.1097/PRS.0b013e3181a20526
2. Gans C, Bock WJ. The functional significance of muscle architecture: A theoretical analysis. *Ergeb Anat Entwicklungsgesch*. 1965;38:115-142.
3. Sacks RD, Roy RR. Architecture of the hind limb muscles of cats: functional significance. *J Morphol*. 1982;173(2):185-195. doi:10.1002/jmor.1051730206
4. Stevoska S, Pisecky L, Stadler C, Gahleitner M, Klasan A, Klotz MC. Tendon transfer in foot drop: a systematic review. *Arch Orthop Trauma Surg*. 2023;143(2):773-784. doi: 10.1007/s00402-021-04162-x
5. Liu AT, Liu BL, Lu LX, Chen G, Yu DZ, Zhu L, Guo R, Dang RS, Jiang H. Architectural properties of the neuromuscular compartments in selected forearm skeletal muscles. *J Anat*. 2014;225(1):12-18. doi: 10.1111/joa.12193. Erratum in: *J Anat*. 2015 May;226(5):497.
6. Lieber RL, Jacobson MD, Fazeli BM, Abrams RA, Botte MJ. Architecture of selected muscles of the arm and forearm: anatomy and implications for tendon transfer. *Hand Surg Am*. 1992;17(5):787-798. doi:10.1016/0363-5023(92)90444-t
7. Lim AY, Kumar PV, Hua J, Pereira BP, Pho RW. The neuromuscular compartments of the flexor carpi ulnaris. *Plast Reconstr Surg*. 1999;103(3):1046-1053.
8. Lim AY, Lahiri A, Pereira BP, Kumar VP, Tan LL. Independent function in a split flexor carpi radialis transfer. *J Hand Surg Am*. 2004;29(1):28-31. doi:10.1016/j.jhsa.2003.09.011
9. Infantolino BW, Challis JH. Architectural properties of the first dorsal interosseous muscle. *J Anat*. 2010;216(4):463-469. doi:10.1111/j.1469-7580.2009.01196.x
10. Butler EE, Dominy NJ. Architecture and functional ecology of the human gastrocnemius muscle-tendon unit. *J Anat*. 2016;228(4):561-568. doi:10.1111/joa.12432
11. Ward SR, Eng CM, Smallwood LH, Lieber RL. Are current measurements of lower extremity muscle architecture accurate? *Clin Orthop Relat Res*. 2009;467(4):1074-1082. doi:10.1007/s11999-008-0594-8
12. Sopher RS, Amis AA, Davies DC, Jeffers JR. The influence of muscle pennation angle and cross-sectional area on contact forces in the ankle joint. *J Strain Anal Eng Des*. 2017;52(1):12-23. doi:10.1177/0309324716669250
13. Kissane RWP, Charles JP, Banks RW, Bates KT. The association between muscle architecture and muscle spindle abundance. *Sci Rep*. 2023;13(1):2830. doi: 10.1038/s41598-023-30044-w
14. Kissane RWP, Charles JP, Banks RW, Bates KT. Skeletal muscle function underpins muscle spindle abundance. *Proc Biol Sci*. 2022;289(1976):20220622. doi:10.1098/rspb.2022.0622
15. Williams SA, Stott NS, Valentine J, Elliott C, Reid SL. Measuring skeletal muscle morphology and architecture with imaging modalities in children with cerebral palsy: a scoping review. *Dev Med Child Neurol*. 2021;63(3):263-273. doi:10.1111/dmcn.14714
16. Lima KM, da Matta TT, de Oliveira LF. Reliability of the rectus femoris muscle cross-sectional area measurements by ultrasonography. *Clin Physiol Funct Imaging*. 2012;32(3):221-226. doi:10.1111/j.1475-097X.2011.01115.x
17. Debernard L, Robert L, Charleux F, Bensamoun SF. Characterization of muscle architecture in children and adults using magnetic resonance elastography and ultrasound techniques. *J Biomech*. 2011;44(3):397-401. doi:10.1016/j.jbiomech.2010.10.025
18. Rana M, Wakeling JM. In-vivo determination of 3D muscle architecture of human muscle using free hand ultrasound. *J Biomech*. 2011;44(11):2129-2135. doi:10.1016/j.jbiomech.2011.05.026
19. Phosphate buffered saline. Protocols Online. 2010. Accessed July 24, 2022. <https://www.protocolsonline.com/recipes/phosphate-buffered-saline-pbs/>
20. Wickiewicz TL, Roy RR, Powell PL, Edgerton VR. Muscle architecture of the human lower limb. *Clin Orthop Relat Res*. 1983;(179):275-283.

21. Fukunaga T, Roy RR, Shellock FG, Hodgson JA, Day MK, Lee PL, Kwong-Fu H, Edgerton VR. Physiological cross-sectional area of human leg muscles based on magnetic resonance imaging. *J Orthop Res.* 1992;10(6):928-934. doi:10.1002/jor.1100100623
22. Bolsterlee B, Finni T, D'Souza A, Eguchi J, Clarke EC, Herbert RD. Three-dimensional architecture of the whole human soleus muscle in vivo. *PeerJ.* 2018;6:e4610. doi:10.7717/peerj.4610
23. Friederich JA, Brand RA. Muscle fiber architecture in the human lower limb. *J Biomech.* 1990;23(1):91-95. doi:10.1016/0021-9290(90)90373-b
24. Pierrynowski MR, Morrison JB. A physiological model for the evaluation of muscular forces in human locomotion: theoretical aspects. *Mathematical Biosciences.* 1985;75(1):69-101. [https://doi.org/10.1016/0025-5564\(85\)90067-7](https://doi.org/10.1016/0025-5564(85)90067-7)
25. Cutts A. The range of sarcomere lengths in the muscles of the human lower limb. *J Anat.* 1988 Oct;160:79-88.
26. Alexander RM. The dimensions of knee and ankle muscles and the forces they exert. *J Hum Move Stud.* 1975;1:115-123.
27. Charles JP, Suintaxi F, Anderst WJ. In vivo human lower limb muscle architecture dataset obtained using diffusion tensor imaging. *PLoS one.* 2019;14(10):e0223531. <https://doi.org/10.1371/journal.pone.0223531>
28. Seth A, Sherman M, Reinbolt JA, Delp SL. OpenSim: a musculoskeletal modelling and simulation framework for in silico investigations and exchange. *Procedia IUTAM.* 2011;2:212-232. doi:10.1016/j.piutam.2011.04.021